J Mater Sci (2007) 42:9409–9414
DOI 10.1007/s10853-007-1888-z

Sintering of ultra-fine tetragonal yttria-stabilized zirconia ceramics

Hwan-Cheol Kim · In-Jin Shon · In-Kyoon Jeong · In-Yong Ko · Z. A. Munir

Received: 19 January 2006 / Accepted: 29 May 2007 / Published online: 27 July 2007

Abstract High-frequency induction heated sintering (HFIHS) is utilized to consolidate ultra-fine grain tetragonal zirconia stabilized with 3 mol%Y_2O_3 (3Y-SZ) ceramics. Densification to near theoretical density in a relatively short time can be accomplished using this method. Samples of 3Y-SZ with a relative density of up to 99.5% and an average grain size of about 170 nm could be obtained by sintering at 950 °C for 5 min under a pressure of 100 MPa pressure. The influence of sintering temperature and mechanical pressure on the final density and grain size of the sintered products was investigated. The sintered materials had fracture toughness and hardness values of 4.4 MPa $m^{1/2}$ and 10.7 GPa, respectively.

Introduction

Yttria-stabilized zirconia (YSZ) has been extensively used as an electrolyte in solid oxide fuel cells (SOFCs) because of its attractive properties, which include high oxygen-ion and low electronic conductivity at high temperatures, stability in both oxidizing and reducing atmospheres, and a relatively economical cost [1–5]. In addition to these, high fracture strength and toughness, excellent thermal conductivity, and good thermal expansion compatibility with other cell components make these materials suitable for are fabrication as self-supported electrolyte plates for use in planar SOFC systems. Such systems have higher volumetric power density than the alternative tubular SOFC systems [1–5]. Cubic zirconia stabilized with 8 mol% yttria (8Y-SZ) is commonly used in SOFC as the electrolyte material due to its high ionic conductivity at high operating temperatures. However, the mechanical strength of 8Y-SZ is relatively poor, adversely affecting the prospect of fabrication of self-supported electrolyte plate for use in planar SOFC [6]. On the other hand, tetragonal zirconia stabilized with 3 mol% Y_2O_3 (3Y-SZ) has a high bending strength at room temperature [7] and a reasonable ionic conductivity at 1000 °C. Although the ionic conductivity of 3 mol% YSZ is lower than that of the 8 mol% YSZ, the advantages in mechanical properties make its consideration attractive for electrolyte material when the cell is designed as an electrolyte support [8].

In order to achieve high ionic conductivity, the material must be prepared in dense and uniform state with a well controlled stoichiometry. Recent studies made on stabilized zirconia have shown that the ionic conductivity may be influenced by the microstructure and the grain size. The total ionic conductivity of 3Y-SZ is mainly influenced by the grain boundaries rather than the grain [9]. A larger number of grain boundaries and the existence of porosity lead to greater resistivity in the fine-grained samples. Additionally, the reduction of grain size also changes the mechanical properties and the sintering behavior of nanocrystalline materials [10, 11]. The sintering temperature of nanocrystalline zirconia is about 400–500 °C lower than for microcrystalline material [12].

H.-C. Kim · I.-J. Shon (✉) · I.-K. Jeong · I.-Y. Ko
Department of Advanced Materials Engineering, Research Center of Advanced Materials Development, Engineering Research Institute, Chonbuk National University, 664-14, Duckijn-Dong, Duckjin-Ku, Jeonju, Jeonbuk 560-756, Republic of Korea
e-mail: ijshon@chonbuk.ac.kr

Z. A. Munir
Facility for Advanced Combustion Synthesis, Department of Chemical Engineering and Materials Science, University of California, Davis, CA 95616, USA

When conventional sintering processes are used to sinter nano-sized zirconia powders, concomitant grain growth leads to the destruction of the nanostructure. This focuses attention on consolidation methods in which grain growth can be eliminated or significantly reduced. To accomplish this, rapid sintering methods have been widely used to sinter nano-sized powders. The most obvious advantage of rapid sintering is that fast heating and cooling rates, and the short dwell time lead to bypassing low-temperature, non-densifying mass transport (e.g., surface diffusion) [13–15]. However, conventional rapid heating can lead to temperature gradients and thus differential densification (non-uniform microstructures), low density, or specimen cracking. To overcome these difficulties, other rapid sintering techniques, such as the spark plasma sintering (SPS) method [16, 17], have been developed.

High-frequency induction heated sintering (HFIHS) is a new rapid sintering method which was developed recently for the fabrication of ceramics and composites [18–21]. This method combines a short time, high-temperature exposure with pressure application. During the HFIHS, a large current will be induced in the sample and in the graphite die. As a result, the sample can be sintered uniformly and rapidly. In this work, we report results on the sintering of 3Y-SZ by the HFIHS method. The goal of this work is to produce dense, ultra-fine 3Y-SZ ceramics in relatively short sintering times. In addition we report on the effect of sintering temperature and mechanical pressure on the sintering behavior and on the mechanical properties of the densified 3Y-SZ materials.

Experimental procedure

The yttria stabilized zirconia powder used in this research was supplied by Nanostructured and Amorphous Materials, Inc. (Houston, TX, USA). The powder had a grain size of 58–76 nm measured by specific surface area (SSA) and was reported to be 99.9% pure. The crystalline phases consisted of 70% monoclinic and 30% tetragonal phase according to supplier's information and as verified by X-ray analysis.

The 3Y-SZ powders were placed in a graphite die (outside diameter, 45 mm; inside diameter, 20 mm; height, 40 mm) and then introduced into the high-frequency induction-heated sintering system (Eltek Co., Korea). A schematic diagram of this method is shown in Fig. 1. The system was first evacuated and a uniaxial pressure of 60 MPa or 100 MPa was applied. An induced current (frequency of about 50 kHz) was then activated and maintained until the densification rate was negligible, as indicating by the observed shrinkage of the sample. Sample shrinkage is measured in real time by a linear gauge

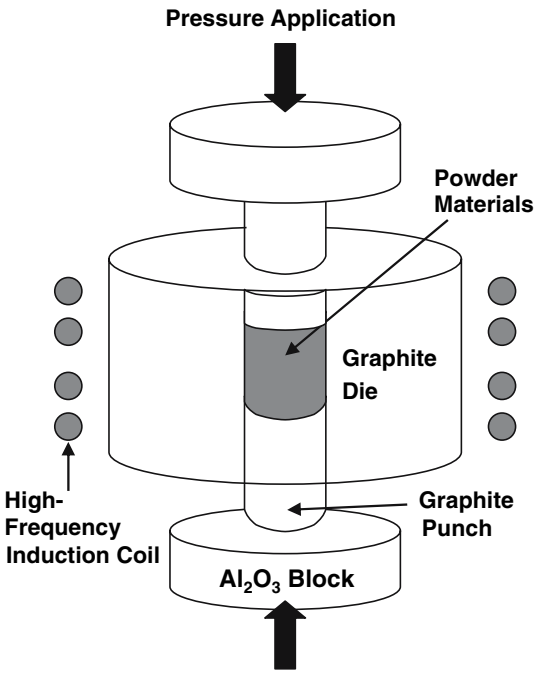

Fig. 1 Schematic diagram of apparatus for high-frequency induction heated sintering

measuring the vertical displacement. Temperatures were measured by a pyrometer focused on the surface of the graphite die. A heating rate of 200 °C/min was used in this study. At the end of the process, the induced current was turned off and the sample was allowed to cool to room temperature. The process was carried out under a vacuum of 4×10^{-2} torr.

The relative densities of the sintered samples were measured by the Archimedes method. Microstructural information was obtained from product samples, which had been polished and fractured. Compositional and microstructural analyses of the products were made through X-ray diffraction (XRD) and scanning electron microscopy (SEM). Vickers hardness was measured by performing indentations at a load of 10 kg_f and a dwell time of 15 s. The oxide grain size, d_{wc} was obtained by the linear intercept method [22, 23].

Results and discussion

The variations of shrinkage displacement and temperature with heating time during the sintering of 3Y-SZ ceramics under 100 MPa pressure and 90% output of total power capacity are shown in Fig. 2. As the induced current is applied, the shrinkage displacement slowly increased with temperature up to about 800 °C, and then abruptly increased as the temperature is further increased from this value. When the temperature reaches 950 °C, the

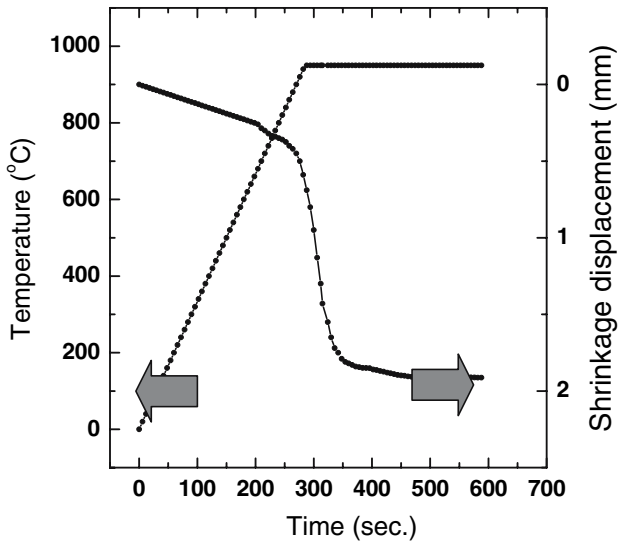

Fig. 2 Variations of temperature and shrinkage displacement with heating time during sintering of 3Y-SZ ceramics (100 MPa pressure, 950 °C for 5 min)

densification rate becomes nearly negligible, and as will be seen later, the samples have densified to 99.8% of theoretical density in about 5 min at 950 °C. The XRD patterns of 3Y-SZ samples before (as-received) and after sintering (as-fractured) at various sintering temperatures (900–1300 °C) are shown in Fig. 3. The sintered samples contained mainly the tetragonal phase of zirconia. The monoclinic phase, present in the initial powder and also in samples sintered at 900 °C (for 5 min) is absent when sintering is done at higher temperatures. Zirconia ceramics consist of three polymorphs; monoclinic, tetragonal and cubic. These phases can be obtained depending on temperature and compositional ranges under equilibrium conditions [24–26]. Monoclinic zirconia is stable phase at room temperature up to 1240 °C. Tetragonal zirconia is stable between 1240 °C and 2370 °C. The retention of the tetragonal phase can be controlled as in the case of cubic zirconia by the addition of dopants. Y_2O_3 additions yield an extremely fine grained microstructure known as tetragonal zirconia polycrystal which has excellent mechanical properties. Cubic zirconia is the highest temperature phase which is present in the temperature range of 2370 ° and 2680 °C. However, upon the addition of a few percent of stabilizers; such as CaO, MgO or Y_2O_3, the cubic phase can be obtained at lower temperatures [24, 25]. The high-temperature cubic phase can also be retained at room temperatures as a non-equilibrium phase by rapid cooling such that diffusive transformation does not occur. The cubic form of stabilized zirconia ceramics are of technological importance due to their high oxygen ionic conductivity at around 1000 °C. Their use as solid state electrolytes has allowed the creation of novel application such as oxygen gas sensors, oxygen membrane separators and solid oxide fuel cells (SOFCs). Increasing the sintering temperature, the crystallite sizes were increased, and FWHM of the sample decreased.

Figure 4 shows the influence of sintering temperature on the product relative density for a constant holding time of 5 min and a heating rate of 200 °C/min for samples sintered under pressure of 60 and 100 MPa. For the case of 60 MPa, the results show that significant densification is obtained only when the temperature is above 1000 °C. The figure also shows the influence of the applied pressure on the density. The higher pressure resulted in higher density as well as lower sintering temperature. Using 100 MPa

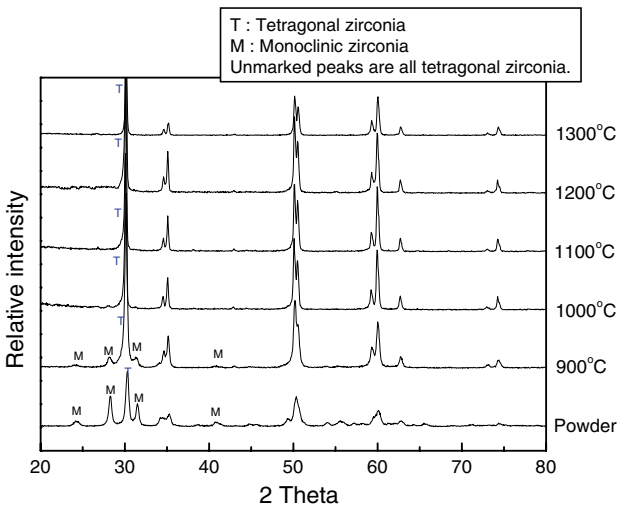

Fig. 3 XRD patterns of 3Y-SZ with various sintering temperatures under 60 MPa

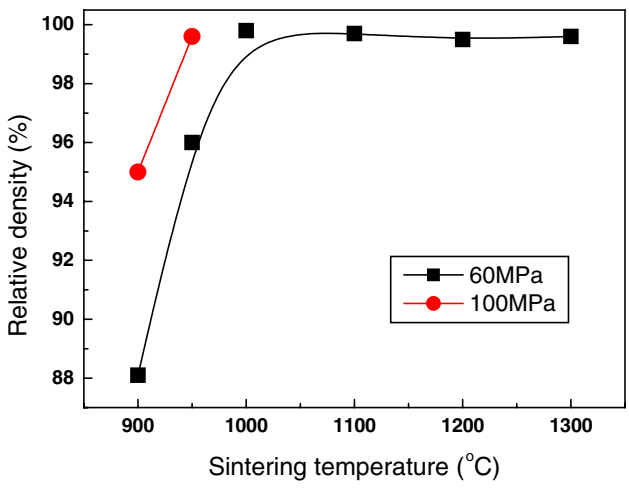

Fig. 4 Relative densities of samples sintered at different temperatures under two levels of applied pressure. The holding time was 5 min and heating rate 200 °C/min

pressure, nearly fully dense sample can be obtained at 950 °C with 5 min holding time.

As the sintering temperature is increased from 900 °C to 1300 °C, an increase in grain size was observed. This is seen from the SEM images of fracture surfaces of samples sintered at various temperatures for 5 min with a pressure of 60 MPa (Fig. 5). As can be seen from this figure, the ZrO_2 grains of the raw materials are generally round and exhibit some agglomeration. The initial particle size measured by linear intercept method and XRD was about 55 and 59 nm, respectively.

The dependence of grain size on sintering temperature is shown in Fig. 6. Grain size of less than about 400 nm could be obtained only at temperatures below 1000 °C. Sintering at higher temperatures resulted in a dramatic increase in grain sizes, and for the highest temperature, 1300 °C, the size is close to 1 μm.

The dense, fine-grained 3Y-SZ ceramics are advantageous as electrolytes in SOFCs by ensuring the absence cross-leakage of fuel and oxidant gases [27]. To reduce the grain size and to increase the density, a higher mechanical pressure of 100 MPa was used. In the case of 60 MPa pressure, it was not possible to obtain the fully dense samples at sintering temperatures below 1000 °C. With a pressure of 100 MPa, however, fully dense samples with grain size about 170 nm could be obtained, as shown in Fig. 7. In the work of Laberty-Robert et al. [28], they obtained had large grain sizes (about 5 μm) for a dwell time of 4 h at 1450 °C under 1 atm using an average crystallite size of 20 nm. The difference between present results and those of Laberty-Robert et al. [28] is related to temperature, pressure and time considerations. Similar

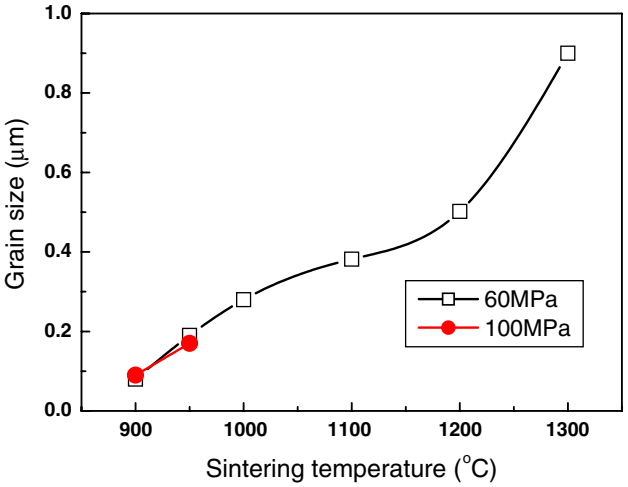

Fig. 6 Dependence of grain size of 3Y-SZ on sintering temperature and applied pressure

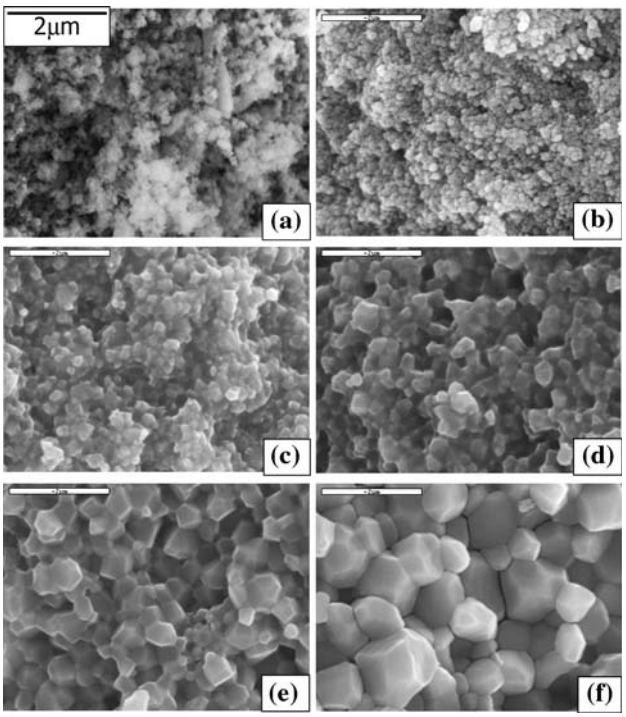

Fig. 5 SEM images of 3Y-SZ (**a**) raw materials, and sintered at (**b**) 900 °C, (**c**) 1000 °C, (**d**) 1100 °C, (**e**) 1200 °C and (**f**) 1300 °C under 60 MPa

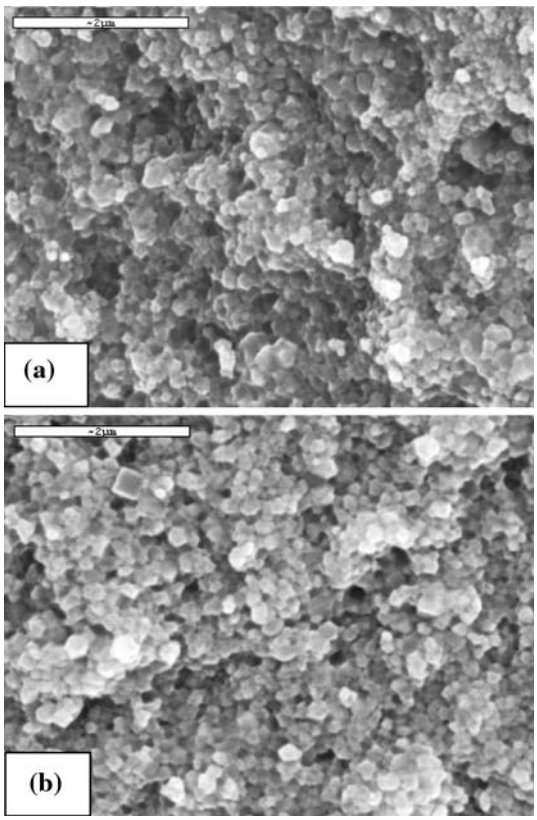

Fig. 7 SEM images of 3Y-SZ sintered at 950 °C (**a**) 60 MPa and (**b**) 100 MPa

considerations may also be offered to explain the difference between the current results and those of Takeuchi et al. [27] who also investigated the sintering of cubic zirconia. They used the YSZ powder with average grain size of 0.1 μm as a starting powder. The YSZ powder was sintered in the form of disks by SPS for 5 min at 1300 °C under 30 MPa or by conventional heating in a muffle furnace for 2 h at 1600 °C. The grain sizes of YSZ obtained by SPS and conventional sintering were about 1 μm and 5 μm, respectively [27].

That the applied pressure has a significant influence on the densification process is clearly demonstrated by results of Fig. 4. At 900 °C, the final relative density of the samples increased from about 88% to about 95% as the applied pressure increased from 60 MPa to 100 MPa. However, Fig. 6 also shows that the pressure has apparently no effect on the grain size over the range investigated, between 60 MPa and 100 MPa. The application of pressure can be added to the surface energy as a driving force for initial-stage densification when multiplied by a dimensional constant (r/π) involving the particle radius [29];

$$F_D = \gamma + (P_a r/\pi) \quad (1)$$

where γ is the surface energy, P_a is the applied pressure, and r is the radius of the particle. This driving force is applicable to all properly formulated initial-stage diffusion models which predict that shrinkage take place. For those models, the occurrence of shrinkage originates with the assumption that the grain boundary acts as the vacancy sink. The effect of pressure on the densification of nanometric, undoped zirconia during sinter-forging was investigated by Skandan et al. [30]. A significant increase in the relative density was observed as the pressure was increased from about 35 MPa to 300 MPa for sintering at 950 °C for 180 min.

To investigate the mechanical properties, Vickers hardness and fracture toughness measurements were made on polished sections of the ZrO_2 ceramics using a 10 kg_f load and 15 s dwell time. The mechanical properties were investigated on samples densified under 60 and 100 MPa with a heating rate of 200 °C/min and a holding time of 5 min at 950 °C. The hardness values obtained under two mechanical pressures are 9.5 GPa and 10.7 GPa, respectively, as shown in Table 1. Indentations with large enough loads produced radial cracks emanating form the corners of the indent. Fracture toughness was calculated from cracks produced in indentations under large loads. From the length of these cracks, fracture toughness values can be determined using two expressions. The first expression, proposed by Anstis et al. [31] is;

$$K_{IC} = 0.016(E/H_v)^{1/2} \cdot P/C^{3/2} \quad (2)$$

where E is Young's modulus (3Y-SZ = 190 GPa), H_v the indentation hardness, P the indentation load, and C the trace length of the crack measured from the center of the indentation. The second expression, proposed by Niihara et al. [32,33];

$$K_{IC} = 0.023(c/a)^{-3/2} \cdot H_v \cdot a^{1/2} \quad (3)$$

where c is the trace length of the crack measured from the center of the indentation, a the half of average length of two indent diagonals, and H_v the hardness. The Niihara relation is appropriate for brittle materials that have relatively low crack-to-indent ratios and because of the crack pattern. Specifically the ratio values should be in the range $0.25 \le c/a \le 2.5$, which is the case for all fracture toughness values reported. The crack pattern was of the Palmqvist mode, as has been also observed by others who also used the relationship described by Eq. 3. For comparison, however, calculations of the fracture toughness were also made using the relationship proposed by Anstis et al.

Typically, one to three additional cracks were observed to propagate radially from the indentation. As in the case of hardness values, the toughness values were derived from the average of five measurements and investigated on samples densified under 60 and 100 MPa at 950 °C for 5 min. The results are also presented in Table 1. Two sets of fracture toughness values are shown in this table, as calculated by the two relationships cited above [31, 32]. The toughness values obtained by the two methods of calculation are 4.4 and 3.0 MPa $m^{1/2}$, respectively. The hardness value increased with increasing the applied pressure without significant change of fracture toughness. It is considered that the improvements in properties are due to the higher density of the samples with similar grain size. The H_v value obtained in this study was a little lower than exhibited by the dense TZP obtained by other methods [34]. It is known that the hardness value of the product depended on the purity and producing method of the raw materials. Using the co-precipitated powder of 3YSZ, we could get the sample with 13.5 GPa of hardness and 5.5 MPa $m^{1/2}$ of toughness produced by high-frequency induction heating sintering method.

Table 1 Hardness and toughness values of 3Y-SZ produced by HFIHS at 950 °C for 5 min

Applied pressure (MPa)	Hardness (GPa)	Toughness (Niihara et al., MPa $m^{1/2}$)	Toughness (Anstis et al., MPa $m^{1/2}$)
60	9.5	4.4	3.1
100	10.7	4.4	3.0

HFIHS have short-time high-temperature exposure with high-pressure applications. The role of the inductive current in sintering and or synthesis has been the focus of several attempts aimed at providing an explanation to the observed enhancement of sintering and improved characteristics of the product. An example of the latter is the observation of clean boundaries in ceramics sintered by HFIHS method relative to those obtained by conventional methods. The role played by the current has been variously interpreted, the effect being explained in terms of fast heating rate due to Joule heating, the presence of plasma in pores separating powder particles, and the intrinsic contribution of the current to mass transport. So we would suggest that the accelerated HFIHS densification may be attributed to a combination of fast heating rates and intrinsic effects on mass transport.

Summary

Using the high-frequency induction heated sintering (HFIHS) method, rapid consolidation of ultra-fine 3 mol% Y_2O_3-stabilised ZrO_2 was accomplished. 3Y-SZ with a relative density up to 99.8% and a grain size of about 170 nm could be obtained with simultaneous application of 100 MPa pressure and induced current. The influence of sintering temperature and mechanical pressure on the final density and grain size of products were investigated. With an increase in the sintering temperature, the relative density and grain size increased. Increasing the applied pressure resulted in a decrease in the required sintering temperature and an increase in the relative density. However, the pressure had no apparent effect on the grain size. The hardness and fracture toughness of the dense ZrO_2 ceramics produced by HFIHS were 10.7 GPa and 4.4 MPa $m^{1/2}$, respectively for sintering with a pressure of 100 MPa at 950 °C for 5 min.

Acknowledgements This work was supported by the grant of Post-Doc. Program, Chonbuk National University (2005). The support of one of us (ZAM) by the Army Office of Research is acknowledged.

References

1. Minh NQ (1993) J Am Ceram Soc 76:563
2. Yamamoto O (2000) Elctrochim Acta 45:2423
3. Badwal SPS, Ciacchi FT, Rajendran S, Drennan J (1982) Solid State Ionics 6:167
4. Mori M, Abe T, Itoh H, Yamamoto O, Takeda Y, Kawahara T (1994) Solid State Ionics 74:157
5. Feighery AJ, Irvine JTS (1999) Solid State Ionics 121:209
6. Khor KA, Yu LG, Chan SH, Chen XJ (2003) J Eur Ceram Soc 23:1855
7. Gupta TK, Lange FF, Bechtold JH (1978) J Mater Sci 13:1464 DOI: 10.1007/BF00553200
8. Yamamoto O, Takeda Y, Imanishi N, Kohno K, Kawahara T (1992) In: Proceedings of international fuel cell conference, 3–6 Feb, 1992. NEDO, Makuhari, p 385
9. Ramamoorthy R, Sundararaman D, Ramasamy S (1999) Solid State Ionics 123:271
10. Verkerk MJ, Middelhuis BJ, Burgraaf AJ (1982) Solid State Ionics 6:159
11. Kim HC, Shon IJ, Garay JE, Munir ZA (2004) Int J Refract Met Hard Mater 22:257
12. Yoshimura M, Ohji T, Sando M, Niihara K (1998) J Mater Sci Lett 17:1389
13. Morell A, Mermosin A (1980) Bull Am Ceram Soc 59:626
14. Chen DJ, Mayo MJ (1996) J Am Ceram Soc 79:906
15. Chen DJ, Mayo MJ (1993) Nanostruct Mater 2:469
16. Omori M (2000) Mater Sci Eng A 287:183
17. Tokita M (1997) Nyu Seramikkusu 10:43
18. Kim HC, Shon IJ, Munir ZA (2005) J Mater Sci 40:2849 DOI: 10.1007/s10853-005-2422-9
19. Kim HC, Oh DY, Shon IJ (2004) Int J Refract Met Hard Mater 22:197
20. Kim HC, Oh DY, Shon IJ (2004) Int J Refract Met Hard Mater 21:41
21. Kim HC, Shon IJ, Yoon JK, Doh JM, Munir ZA (2006) Int J Refract Met Hard Mater 24:427
22. Astm E112-96e2
23. Han JH, Kim DY (1998) Acta Mater 46:2021
24. Grain CF (1967) J Am Ceram Soc 50:288
25. Scott HG (1975) J Mater Sci 10:1527 DOI: 10.1007/BF01031853
26. Kazutaka S (2001) Ph.D. Thesis, Tokyo University
27. Takeuchi T, Kondoh I, Tamari N, Balakrishnan N, Nomura K, Kageyama H, Takeda Y (2002) J Electrochem Soc 149:A455
28. Laberty-Robert C, Ansart F, Deloget C, Gaudon M, Rousset A (2003) Ceram Int 29:151
29. Coble RL (1970) J Appl Phys 41:4798
30. Skandan G, Hahn H, Kear BH, Roddy M, Cannon WR (1994) Mater Lett 20:305
31. Anstis GR, Chantikul P, Lawn BR, Marshall DB (1981) J Am Ceram Soc 64:533
32. Niihara K (1985) Ceramics 20:1218
33. Oh DY, Kim HC, Yoon JK, Shon IJ (2005) J Alloys Compd 395:174
34. Basu B, Vleugels J, Van Der Biest O (2004) J Eur Ceram Soc 24:2031